Nonconformal Potentials and Second Virial Coefficients in Molecular Fluids. II. Applications to Nonspherical Molecules

J. Eloy Ramos and Fernando del Río*

Departamento de Física, Universidad Autónoma Metropolitana Iztapalapa, Apdo 55 534, México DF, 09340, México

Ian A. McLure

Department of Chemistry, University of Sheffield, Sheffield, S3 7HF, U.K.

Received: February 6, 1998; In Final Form: July 23, 1998

A theory recently proposed characterizes effective two-body interactions in gases by molecular sizes and energies plus effective measures of the nonconformality between the exact potential and a spherical reference. This theory provides a procedure to construct effective potentials which reproduce the second virial coefficients $B(T)$ of the substance of interest and allows us to express $B(T)$ in simple and compact form. In this paper we test the applicability of the theory to a variety of nonspherical models—spherocylinders, ellipsoids, Lennard−Jones polyatomics, square-well chains, and Stockmayer molecules—and show that their virial coefficients are accounted for accurately by the theory. The theory is used to study the effects of molecular geometry, particularly the elongation of linear molecules, on the angle averaged molecular parameters and on the effective potential. The effective potentials of the models considered are obtained, and the effects of size and geometrical shape are discussed.

1. Introduction

In a recent paper, we proposed a theory to take into account the nonconformality of two potential functions in the prediction of thermodynamic properties of dilute gases.[1] This theory provides an explanation of regularities in the behavior of second virial coefficients $B(T)$ and mean collision diameters found previously.[2] We have shown that effective pair intermolecular potentials are characterized by two scale parameters—a distance r_m and an energy ϵ—and two constants S_R and S_A describing the softness of the potential of interest in its repulsive and attractive regions with respect to a reference. The theory also provides closed and simple expressions for $B(T)$ of many gases of interest, both model and real. The approach provides a general and simple expression for $B(T)$ and reliable effective pair interaction parameters for many substances, spherical and quasi-spherical, which reproduce the available data within estimated experimental errors.[2]

In this paper, we apply the theory to more complex molecules. Effective potentials are obtained for a variety of nonspherical models—spherocylindrical and ellipsoidal square wells, linear Kihara molecules, multicentered Lennard−Jones, square-well chains, and Stockmayer polar molecules—and the effects of geometrical shape are discussed in light of the theory. The theoretical expressions for $B(T)$, involving at most four constant parameters and the properties of the reference fluid, reproduce with high accuracy the virial coefficients of the models studied. These applications confirm the usefulness of the concepts introduced and illustrate the scope of the approach.

In section 2, we present the main elements of the theory in relation to $B(T)$, and section 3 is devoted to the application of the theory to several nonspherical model systems of wide interest. These applications allow us to explore the limits of applicability of the theory and to analyze the effect of changing various features of the molecular interaction on the effective potential. We explore the effect of deviations from sphericity on the softness parameters describing the nonconformality between the potential of interest and the reference. Special attention is given to the effect of varying the elongation of linear and chain molecules. Last, in section 4 the principal conclusions of this work are summarized.

2. Theory

Here we briefly describe the theory. Full details are given in ref 1. The intermolecular potential is $u(r,\Omega)$ with minimum $u(r_\Omega,\Omega) = -\epsilon_\Omega$ at $r = r_\Omega$. The reduced second virial coefficient is given by the modified square-well expression

$$B^*(T^*) = \frac{B(T^*)}{4b_m} = b^*(T^*)e^{\beta\epsilon} - \Lambda^*(T^*)(e^{\beta\epsilon} - 1) \quad (2.1)$$

with effective range λ_{ef} given by

$$\lambda_{ef}^{\ 3} = \frac{\Lambda^*(T^*)}{b^*(T^*)} \quad (2.2)$$

In eq 2.1, $\beta = 1/kT$, $b_m = \pi r_m^3/6$, r_m, and ϵ are the angle averages of r_Ω and ϵ_Ω defined by

$$r_m^{\ 3} = \int d\Omega\, r_\Omega^{\ 3}(\Omega) = \langle r_\Omega^{\ 3}\rangle_\Omega \quad (2.3)$$

and

$$\epsilon = \langle \epsilon_\Omega \rangle_\Omega \quad (2.4)$$

where the angles Ω are normalized so that $\int d\Omega = 1$. The second virial coefficient (eq 2.1) is determined by the reduced core volume b^* given by

10.1021/jp981040g CCC: $15.00
Published on Web 11/10/1998

$$b^*(T^*)e^{\beta\epsilon} = \int d\Omega\, z_\Omega{}^3 e^{\beta\epsilon_\Omega} - 3\int d\Omega \int_0^{z_\Omega} dz\, z^2 e^{-\beta u(z,\Omega)} \tag{2.5}$$

and by the attractive volume

$$\Lambda^*(T^*)(e^{\beta\epsilon} - 1) = \int d\Omega\, z_\Omega{}^3(e^{\beta\epsilon_\Omega} - 1) + 3\int d\Omega \int_{z_\Omega}^{\infty} dz\, z^2[e^{-\beta u(z,\Omega)} - 1] \tag{2.6}$$

In these equations, $z = r/r_m$, $z_\Omega = r_\Omega/r_m$, and $T^* = 1/\beta\epsilon$. These effective volumes are rewritten in a way suitable to reflect the shape of the potential profile by a transformation used by Frisch and Helfand[3] and Cox et al.;[4] we introduce $\phi(z,\Omega) = u(z,\Omega)/\epsilon + 1$ and change the independent variable from z to ϕ. For potentials whose depth $\epsilon_\Omega = \epsilon$ is independent of Ω, we find from eqs 2.5 and 2.6 the expressions

$$b^* = 1 + \int d\Omega \int_0^{\infty} d\phi \left[\frac{\partial z^3(\phi,\Omega)}{\partial\phi}\right]_R e^{-\beta\epsilon\phi} \tag{2.7}$$

and

$$\Lambda^* = 1 + \frac{1}{e^{\beta\epsilon} - 1}\int d\Omega \int_0^1 d\phi \left[\frac{\partial z^3(\phi,\Omega)}{\partial\phi}\right]_A (e^{-\beta\epsilon(\phi-1)} - 1) \tag{2.8}$$

where $z(\phi,\Omega)$ is the inverse of $\phi(z,\Omega)$ in the repulsive and attractive regions of $\phi(z)$ denoted here by the indexes R and A, respectively. The nonconformality between $u(z,\Omega)$ and the reference potential $u_0(z)$ of depth equal to ϵ is accounted for by the softness function $s(\phi,\Omega)$

$$s(\phi,\Omega) = \frac{\epsilon_\Omega[\partial u_0(z)/\partial z^3]_{z_0(\phi)}}{\epsilon[\partial u(z,\Omega)/\partial z^3]_{z(\phi)}} \tag{2.9}$$

Here we take the spherical Kihara potential as a reference

$$u_0(z)/\epsilon_0 = \left[\frac{1-a}{z-a}\right]^{12} - 2\left[\frac{1-a}{z-a}\right]^6 \tag{2.10}$$

where a is the hard-core diameter in units of r_m. We further take $a = 0.0957389$ so that $u_0(z)$ is a good representation of the pair potential of argon.

When s_R and s_A are independent of ϕ, we define

$$S_R = \langle s_R\rangle_\Omega \tag{2.11}$$

and similarly $S_A = \langle s_A\rangle_\Omega$. It has been shown that using eqs 2.9, 2.10, and 2.11 in eqs 2.7 and 2.8, the effective volumes can be expressed by[1]

$$b^*(T^*) = 1 - S_R + S_R b_0^*(T^*) \tag{2.12}$$

and

$$\Lambda^*(T^*) = 1 - S_A + S_A\Lambda_0^*(T^*) \tag{2.13}$$

where b_0^* and Λ_0^* are the reference volumes. Then the virial coefficient in eq 2.1 becomes

$$B^*(T^*) = [1 - S_R + S_R b_0^*(T^*)]e^{\beta\epsilon} - [1 - S_A + S_A\Lambda_0^*(T^*)](e^{\beta\epsilon} - 1) \tag{2.14}$$

which when $S_R = S_A = S$ simplifies into

$$B^*(T^*) = 1 - S + SB_0^*(T^*) \tag{2.15}$$

In the cases when s_R and s_A depend on ϕ or when ϵ_Ω depends on the angles, eqs 2.12 and 2.13 hold as approximations.[1] The effective potential has a well-defined softness with respect to the reference (eq 2.10) and has the modified Kihara form

$$u_{MK}(z;S) = \epsilon\left[\frac{1-a}{(z^3/S + 1 - 1/S)^{1/3} - a}\right]^{12} - 2\epsilon\left[\frac{1-a}{(z^3/S + 1 - 1/S)^{1/3} - a}\right]^6 \tag{2.16}$$

When $S_R \neq S_A$, the effective potential is given by

$$u_{ef}(z) = \begin{cases} u_{MK}(z;S_R), & z \le 1 \\ u_{MK}(z;S_A), & z > 1 \end{cases} \tag{2.17}$$

Therefore, to construct the effective potential, one only needs the two scale parameters ϵ and r_m together with the form factors S_R and S_A. In the next section, we apply this theory to a variety of nonspherical potential models of interest and find the corresponding parameters. In each of the cases considered, $u_{ef}(z)$ has the form given by eqs 2.16 and 2.17.

3. Application to Nonspherical Molecules

We now calculate the effect of the shape of the molecules on $b^*(T)$, $\Lambda^*(T)$, and $B^*(T)$. We will discuss several important nonspherical model systems which illustrate the main features of the theory reviewed in the previous section. We start by considering nonspherical hard bodies surrounded by nonspherical SW shells and then move on to continuous and more realistic potentials.

We will consider model molecules whose shape can be represented in terms of a nonspherical body. The size of the body is described in terms of a basic length h and its geometry by a set of dimensionless parameters ξ, such as the elongation of a linear molecule. Let $l(h,\xi,\Omega)$ be the distance l between the centers of two such bodies when they are in contact and their relative orientation is Ω. We consider an interaction which has a fixed value ϵ_h when the two bodies touch, i.e., when

$$r = l(h,\xi,\Omega) \tag{3.1}$$

Among the interactions that can be constructed using eq 3.1 is the hard body (HB) interaction

$$u_{HB}(r,\Omega,\xi,h) = \begin{cases} \infty, & r < l(h,\xi,\Omega) \\ 0, & l(h,\xi,\Omega) > r \end{cases} \tag{3.2}$$

3.1. Nonspherical Square Wells. We will deal with potentials obtained from eq 3.1 by assuming a collection of shells or layers, all of similar geometrical shape but of different thickness h and such that ϵ_h changes from one layer to the next. An important system is the nonspherical square well (NSW)

$$u_{nsw}(r,\Omega) = \begin{cases} \infty & r < l_c(\Omega) \\ -\epsilon & l_c(\Omega) < r < l_u(\Omega) \\ 0 & l_u(\Omega) < r \end{cases} \tag{3.3}$$

where $l_c = l(h_c,\xi_c,\Omega)$ is the nonspherical hard core and $l_u = l(h_u,\xi_u,\Omega)$ is the shell where the attractive force acts. The parameters (h_c,ξ_c) and (h_u,ξ_u) define the geometries of the core and the attractive shell, respectively. The hard core is surrounded by an attractive shell of constant depth ϵ and width $l_u(\Omega) - l_c(\Omega)$. For this potential, the Boltzmann factor in eqs

2.5 and 2.6 is expressed in terms of the Heaviside function as

$$e^{-\beta u(r,\Omega)} = H(r - l_c(\Omega))e^{\beta\epsilon} + H(r - l_u(\Omega))(1 - e^{\beta\epsilon})$$

so that

$$\frac{\partial e^{-\beta u(r,\Omega)}}{\partial r} = \delta(r - l_c(\Omega))e^{\beta\epsilon} + \delta(r - l_u(\Omega))(1 - e^{\beta\epsilon})$$

Integrating eqs 2.5 and 2.6 by parts and over the angles, the mean collision diameters are found to be

$$\sigma^3 = \langle l_c^{\,3}(\Omega)\rangle_\Omega \tag{3.4}$$

$$R^3 = \langle l_u^{\,3}(\Omega)\rangle_\Omega \tag{3.5}$$

The thickness h_c of the core is taken here as the unit of length so that eqs 3.4 and 3.5 give

$$b^*(h_c,\xi_c) = (\sigma/h_c)^3 \tag{3.6}$$

$$\Lambda^*(h_u,\xi_u) = (R/h_c)^3 \tag{3.7}$$

In this case, b^*, Λ^*, and λ_{ef}, given by eq 2.2, are constant with temperature but depend on the geometry through ξ_c and ξ_u.

The following treatment can be easily applied to bodies with hard cores for which the second virial coefficient is known. Such bodies include hard convex bodies and hard dumbbells.[5,6] The volume b^* of the hard body (HB) of thickness h and dimensionless shape parameters ξ is given by

$$b_{hb}^* = \frac{V_{1+2}}{4\pi h^3/3}$$

where V_{1+2} is the covolume of the body written in terms of its volume V, surface area A, and mean curvature integral R as

$$V_{1+2} = 2(V + AR)$$

The geometric functionals V, A, and R are given in terms of h and ξ.[6] Then the volume of the core is

$$b_c^* = b_{hb}^*(\xi_c) \tag{3.8}$$

where ξ_c are the core parameters. In the same way, the volume for the attractive shell of thickness h_u and shape parameters ξ_u will be

$$\Lambda^* = (h_u/h_c)^3 b_{hb}^*(\xi_u) \tag{3.9}$$

The second virial coefficient of the nonspherical square well $B_{nsw}^*(T^*)$ is obtained by substituting eqs 3.8 and 3.9 in eq 2.1. Hence, $B_{nsw}^*(T^*)$ is identical to $B^*(T^*)$ of a spherical SW whose range is obtained from eq 2.2 as

$$\lambda_{nsw}^{\,3} = \lambda_0^{\,3} b_{hb}^*(\xi_u)/b_{hb}^*(\xi_c) \tag{3.10}$$

where $\lambda_0 = h_u/h_c$.

We take as an example a prolate spherocylindrical square well (SCSW): the core and attractive shell are spherocylinders (SC) of diameters h_c and h_u and cylindrical lengths L_c and L_u, respectively. The well has a constant depth ϵ. The geometric parameters are the elongations of the core $\xi_c = L_c^* = L_c/h_c$ and of the attractive shell $\xi_u = L_u^* = L_u/h_u$. The core elongation L_c^* will be used as the principal elongation. From the covolume of a HSC,[6] we find the core volume (eq 3.8)

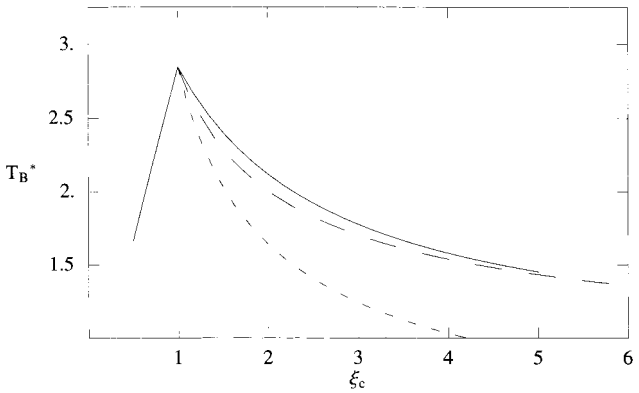

Figure 1. Boyle temperature of nonspherical square-well particles with SW range $\lambda_0 = 1.5$ as function of eccentricity ξ_c. Solid line: oblate ($\xi_c < 1$) and prolate ($\xi_c > 1$) ellipsoids. Long-dashed line: prolate spherocylinders. Short-dashed line: oblate spherocylinders.

$$b_{scsw}^*(L_c^*) = b_{hsc}^*(L_c^*) = \frac{b_{hsc}}{h_c^{\,3}} = 1 + \frac{3}{2}L_c^* + \frac{3}{8}L_c^{*2} \tag{3.11}$$

For the attractive shell we find its volume from eq 3.9 to be

$$\Lambda_{scsw}^*(L_u^*) = \lambda_0^{\,3} b_{hsc}^*(L_u^*) \tag{3.12}$$

where $\lambda_0 = h_u/h_c > 1$ is the SW range for the spherical case $L_c^* = L_u^* = 1$. The SCSW virial coefficient is found by substituting eqs 3.11 and 3.12 in eq 2.1. From eq 3.10, the effective SW range is obtained as

$$\lambda_{scsw}^{\,3} = \lambda_0^{\,3} b_{hsc}^*(L_u^*)/b_{hsc}^*(L_c^*) \tag{3.13}$$

From eq 3.6, the effective core diameter $\sigma \propto b^{*1/3}$, and hence, for large L_c^*, we find that $\sigma \propto (L_c^*)^{2/3}$. This behavior arises from the fact that the covolume for any hard body with cylindrical symmetry grows proportionally to the square of its length. Linear molecules are usually modeled by assigning the same length to both cylinders, i.e., $L = L_u = L_c$, then $L_u^* < L_c^*$ and since $b_{hsc}^*(L^*)$ increases with L^*, we find that λ_{scsw} is smaller than λ_0 and decreases when L^* grows. Thus, such an elongated SCSW has a narrower effective well than the spherical SW of the same λ_0: as L^* increases, the net effect of the attractive forces diminishes and the Boyle and critical temperatures are lower. Figure 1 shows the decrease in the Boyle temperature T_B^* with eccentricity $\xi_c = L^* + 1$ for prolate SCSW with $L_u = L$ and $\lambda_0 = 1.5$.

The same general behavior is found for prolate ellipsoids of revolution. In this case, $l_c(\Omega)$ in eq 3.3 describes the core ellipsoid with minor axis h_c, major axis of revolution L_c, and eccentricity $\xi_c = L_c/h_c$. The outer ellipsoid has h_u and L_u as axes and eccentricity $\xi_u = L_u/h_u$. In modeling linear molecules with two prolate ellipsoids, the range of the well is taken again as the ratio $\lambda_0 = h_u/h_c > 1$ and $L_u = L_c + h_c(\lambda_0 - 1)$. The second relation is equivalent to $\xi_u\lambda_0 = \xi_c + \lambda_0 - 1 > \xi_c$ and ensures that the width of the attractive well is kept constant when the eccentricity ξ_c is increased. To obtain the virial coefficient (eq 2.1), we use again eqs 3.8 and 3.9 with $b_{hb}^*(\xi)$ obtained from the covolume of hard ellipsoids of eccentricity ξ. The effective SW range is given by eq 3.10 and is also found to decrease with increasing ξ_c, so that again, the net effect of the attractive forces is reduced. A similar effect is found for oblate spherocylindrical and ellipsoidal SW particles as their shape departs from spherical and the width of the SW is kept constant. The Boyle temperature for all these systems is also

shown in Figure 1 in terms of the eccentricity ξ_c, for the oblate SC $\xi_c = (h_c + L)/L > 1$ and for the oblate ellipsoid $\xi_c = L_c/h_c < 1$ with L_c as the (minor) axis of revolution. In all cases, departures from sphericity produce narrower effective wells and lower T_B*.

Analysis of these simple nonspherical SW particles allows us to draw an interesting qualitative prediction. For geometrical reasons, deviations from the spherical shape produce a narrower effective well. This will also happen when the core is not convex, as for fused hard spheres, and when the potential is more realistic, i.e., when its repulsive and attractive parts have a finite softness. Further, a narrower attractive well means that $u(z)$ has a steeper slope when plotted against z. Hence, a molecule will appear to be harder the more its shape departs from spherical.

3.2. Linear Molecules. We now consider particles interacting through potentials more realistic than the nonspherical SW. For a given orientation Ω and distance r between the molecules, the layers touching each other have a thickness $h_r = h(r,\Omega,\xi)$ and the value of $u(r,\Omega)$ will be a function of h_r:

$$u(r,\Omega) = \epsilon(h_r)$$

We will concentrate on linear molecules, i.e., particles of spherocylindrical (SC) shape with a smooth potential profile with repulsive and attractive parts, and analyze the relation between the elongation of the molecule and the softness of each part. First, we will obtain general relations pertaining to the SC shape and then particularize to a Kihara potential profile.

The potential between two such particles $u(r,\Omega,L)$ has a constant minimum $-\epsilon$ at a surface $r_\Omega = r(\Omega,L)$. The potential between two SC is taken as $u_0(r)$ when their axes are perpendicular to **r**, the center-to-center vector; this will be called the reference orientation Ω_0. $u_0(r)$ is identical to the potential when the SC has zero elongation and has its minimum at $r = r_0$.

First, we analyze the behavior of $s(\phi,\Omega)$ with Ω. For the reference orientation, we find that the slope ratio in eq 2.9 is $s(\phi,\Omega_0) = 1$. At any orientation $\Omega \neq \Omega_0$, r_Ω will be greater than r_0, and hence, when scaling the distances r with r_Ω to obtain the reduced potential $u(z,\Omega)/\epsilon$ with $z = r/r_\Omega$, the potential profile will become steeper and the softness will decrease. The smaller value s_{min} of $s(\phi,\Omega)$ will occur for the orientation giving the maximum r_Ω, i.e., the end-to-end configuration. Thus, the average softness $S = \langle \bar{s}(\Omega)\rangle_\Omega$ satisfies $s_{min} < S < 1$.

The effective r_m is obtained from the covolume of two spherocylinders of length L and breath r_0. The elongation of these spherocylinders is $L^* = L/r_0$, and hence, its effective volume is from eq 3.6.

$$b_m = \frac{\pi}{6} r_m{}^3 = \frac{\pi}{6}\langle r_\Omega{}^3\rangle_\Omega$$

Following the analysis in the last section, we can write

$$b_m = \frac{\pi}{6} r_0{}^3 b_{hsc}{}^*(L^*)$$

so that

$$\left(\frac{r_m}{r_0}\right)^3 = b_{hsc}{}^*(L^*)$$

The virial coefficient reduced with $4b_m$ is written as

$$B^* = b_{sc}{}^*(T^*,L^*)e^{\beta\epsilon} - \Lambda_{sc}{}^*(T^*,L^*)(e^{\beta\epsilon} - 1) \quad (3.14)$$

The effective volumes b_{sc}* and Λ_{sc}* are obtained by generalizing the discontinuous case treated in the last section. The procedure is straightforward and is outlined in the Appendix. The final result is

$$b_{sc}{}^* = \frac{1}{b_{hsc}{}^*(L^*)}\left[b_0{}^*(T^*) + \frac{3}{2}L^* b_1{}^*(T^*) + \frac{3}{8}L^{*2} b_2{}^*(T^*)\right] \quad (3.15)$$

and

$$\Lambda_{sc}{}^* = \frac{1}{b_{hsc}{}^*(L^*)}\left[\Lambda_0{}^*(T^*) + \frac{3}{2}L^* \Lambda_1{}^*(T^*) + \frac{3}{8}L^{*2} \Lambda_2{}^*(T^*)\right] \quad (3.16)$$

In these equations

$$b_k{}^*(T^*) = 1 - \int_{z_0}^{1} dz^{3-k}\, e^{-\beta u_0(z) - \beta\epsilon}$$

where $z_0 < 1$ is the hard-core diameter of $u_0(z)$ and

$$\Lambda_k{}^*(T^*) = 1 + \int_1^{\infty} dz^{3-k}\, \frac{e^{-\beta u_0(z)} - 1}{e^{\beta\epsilon} - 1}$$

b_0* and Λ_0* are the effective volumes of the spherical body with potential $u_0(r)$. The functions b_k* and Λ_k* were integrated numerically to obtain the volumes $b_{sc}{}^*(T^*)$ and $\lambda_{sc}{}^*(T^*)$ from eqs 3.15 and 3.16 for various elongations and choosing $u_0(r)$ as the spherical Kihara eq 2.10, and the results obtained are shown in Figure 2 for SC of different elongations L^*. It can be shown after a lengthy derivation that eqs 3.14, 3.15, and 3.16 are exactly equivalent to the formula for linear SC molecules obtained by Kihara.[5] As in the case of the simpler SCSW dealt with in the last section, a longer molecule means a larger b_{sc}* and a smaller Λ_{sc}*. We further notice that b_{sc}* and Λ_{sc}* change more slowly with T^* for the more elongated SSC, which thus effectively appear to be harder. These results are also shown in Figure 3 as parametric plots against $b_0{}^*(T^*)$ and $\Lambda_0{}^*(T^*)$ from which we see that they follow closely the linear behavior in eqs 2.12 and 2.13. Results for $b_{sc}{}^*(T^*)$ and $\Lambda_{sc}{}^*(T^*)$ can be obtained easily also for other convex shapes following the procedure in the Appendix.

To explicitly find the dependence of S_R and S_A on L^* for the Kihara SC, numerical calculation of b_k* and Λ_k* shows that we can write to a very good approximation

$$b_k{}^*(T^*) \cong \theta_0 - \alpha_k + \alpha_k b_0{}^*(T^*),\ k = 1, 2$$

$$\Lambda_k{}^*(T^*) \cong \theta_k - \gamma_k + \gamma_k \Lambda_0{}^*(T^*),\ k = 1, 2$$

where $\theta_0 = 1.0111975$, $\theta_1 = 1.059139$, $\theta_2 = 1.04386$, $\alpha_1 = 0.750231$, $\alpha_2 = 0.423182$, $\gamma_1 = 0.456922$, and $\gamma_2 = 0.166949$. These values were obtained from straight-line fits to graphs of b_k* against b_0* and of Λ_k* against Λ_0*. On account of this, eqs 3.15 and 3.16 simplify into linear relations almost identical to eqs 2.12 and 2.13, i.e.

$$b_{sc}{}^*(T^*,L^*) \cong \frac{1 + \theta_0(b_{hsc}{}^* - 1)}{b_{hsc}{}^*} - S_R(L^*) + S_R(L^*) b_0{}^*(T^*) \quad (3.17)$$

and

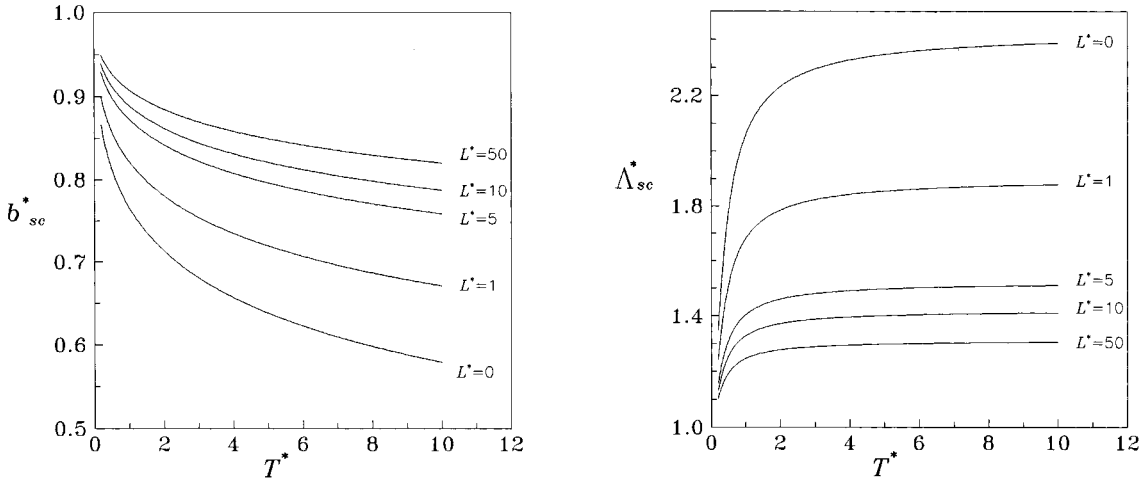

Figure 2. Effective volumes (a) b_{sc}* and (b) Λ_{sc}* of linear Kihara molecules as a function of temperature for various elongations L*. For zero elongation, the particles are identical to the reference $u_0(z)$ in eq 2.10.

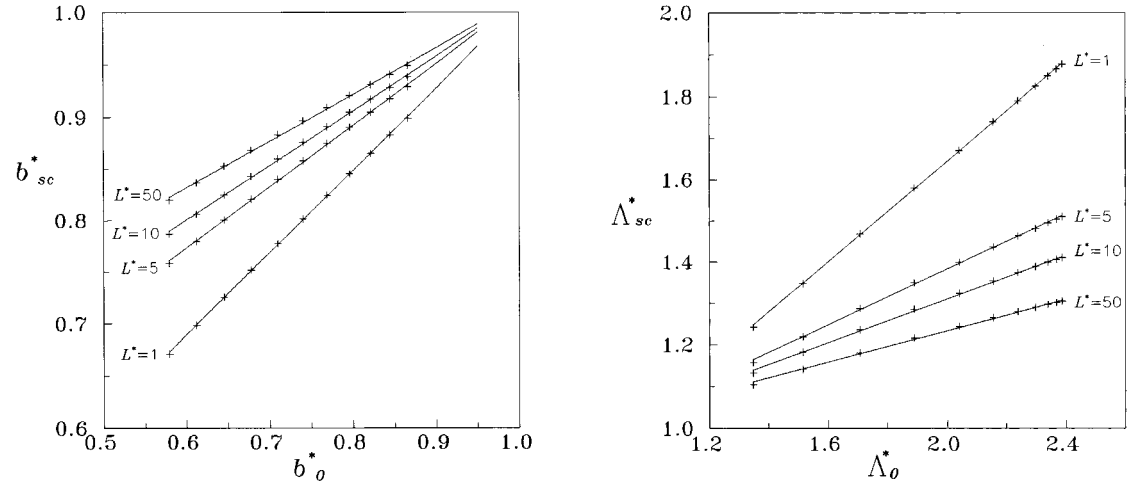

Figure 3. Parametric plots of the effective volumes (a) b_{sc}*(T*) and (b) Λ_{sc}*(T*) of linear Kihara molecules with various elongations L* against the $L^* = 0$ references b_0*(T*) and Λ_0*(T*), respectively. The crosses are the values calculated numerically from eq 3.15 and 3.16. The straight lines are linear fits such as eqs 3.17 and 3.18 to the numerical values.

$$\Lambda_{sc}^*(T^*,L^*) \cong \frac{1 + 3\theta_1 L^*/2 + 3\theta_2 L^{*2}/8}{b_{hsc}^*} - S_A(L^*) + S_A(L^*)\Lambda_0^*(T^*) \quad (3.18)$$

Figure 3 also shows that relations 3.17 and 3.18 are very good approximations indeed. In eqs 3.17 and 3.18, the softness parameters are given by

$$S_R(L^*) = (1 + 3\alpha_1 L^*/2 + 3\alpha_2 L^{*2}/8)/b_{hsc}^* \quad (3.19)$$

$$S_A(L^*) = (1 + 3\gamma_1 L^*/2 + 3\gamma_2 L^{*2}/8)/b_{hsc}^* \quad (3.20)$$

From Figure 4, which shows S_R and S_A calculated directly from the slopes of the lines in Figure 3 and also the plots of eqs 3.19 and 3.20, we see that these equations provide an excellent approximation. In this case of linear Kihara molecules, the exact effective potential at any orientation Ω is a spherical Kihara whose core diameter a depends on L* and Ω. The softnesses $S_R(a)$ and $S_A(a)$ of the spherical Kihara potentials with respect to u_0 have been calculated previously.[1] In the end-to-end configuration, where $S = S_{min}$, we find

$$a(L^*) = \frac{1 + L^*}{1/a_0 + L^*}$$

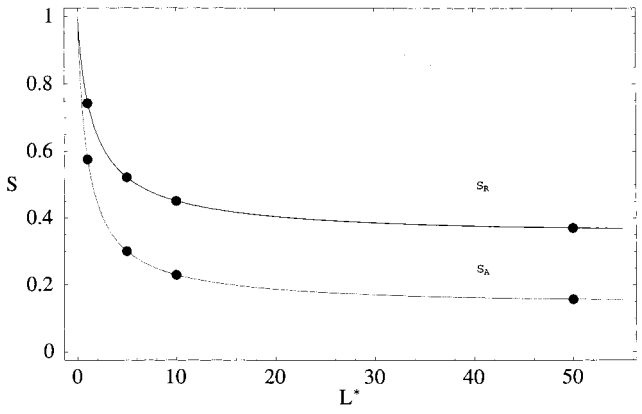

Figure 4. Softness S_R and S_A of linear Kihara molecules as a function of elongation L*. The solid lines are plots of eqs 3.19 and 3.20. The black circles are the values obtained directly from fitting eqs 3.14, 3.17, and 3.18 to numerical values of $B(T)$.

From eqs 3.19 and 3.20 and Figure 4 of ref 1, it can be verified that indeed $S_{min}(L^*) < S(L^*) < 1$.

Hence, the theory with two constant softness parameters works accurately for this realistic model of linear molecules. We find that the softness indeed decreases monotonically with growing elongation, in agreement with the general inference drawn from the simpler SW nonspherical systems.

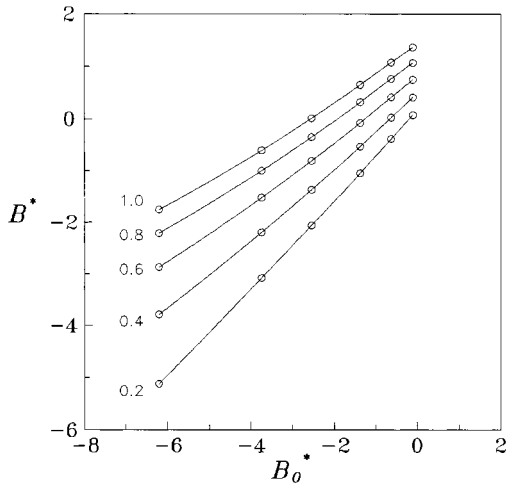

Figure 5. Second virial coefficient $B_{2CLJ}^*(T^*,L^*)$ of two-center Lennard−Jones 12/6 diatomics in a parametric plot against the reference $B_0^*(T^*)$. The elongations are $L^* = L/\sigma_{LJ}$, where L is the internuclear distance and σ_{LJ} is the LJ distance parameter. Circles: numerical values from Maitland et al.[7] and Boublík.[8] Solid line: this theory.

3.3. Multicentered Lennard−Jones Molecules. We now consider an example of a nonspherical model in which the potential minimum, ϵ_Ω, depends on the intermolecular orientation. For this we take the n-center Lennard−Jones 12/6 potential, nCLJ, in which the interaction between two atoms in different molecules, with n atoms each, is the common LJ 12/6 potential. The virial coefficient for this model has been calculated for linear polyatomics $n = 2$, 3, and 4[7,8] of various elongations $l^* = l/\sigma_{LJ}$, where l is the internuclear distance between adjacent atoms in the molecule and σ_{LJ} is the usual LJ parameter. The molecular elongation is then $L^* = (n - 1)l^*$.

Since in the 2CLJ models the depth ϵ_Ω depends strongly on orientation, they provide a harder and wider test of the theory. Here we test whether the basic set of equations (2.12, 2.13, and 2.1) holds for these models and also whether the expectations about the behavior of the parameters are fulfilled; first, since $r_m = \langle r_\Omega \rangle$, it should increase with L^* due to a larger l^* or n and for large L^*, we expect $r_m \propto L^{*2/3}$. Second, at fixed n, the effective depth ϵ should decrease with l^* from its maximum value at $l^* = 0$, where $\epsilon = n^2\epsilon_{LJ}$ and ϵ_{LJ} is the atom−atom LJ energy, to its minimum value at $l^* = \infty$, where $\epsilon = \epsilon_{LJ}$. Third, both S_R and S_A should decrease monotonically with L^* in a manner similar to eqs 3.19 and 3.20 for the SC.

TABLE 1: Parameters of Effective Potentials of Multicentered LJ

n	l^*	r_m	ϵ	S_R	S_A	$Q \times 10^4$
2	0.0	0.995 17	0.993 40	1.069 49	1.194 35	6.3
	0.1	1.007 47	0.951 17	1.059 86	1.176 91	7.1
	0.2	1.037 23	0.865 18	1.039 64	1.125 57	8.2
	0.3	1.075 73	0.779 87	1.021 67	1.053 15	1.0
	0.4	1.116 89	0.707 18	1.006 61	0.980 97	13
	0.5	1.159 29	0.646 57	0.997 93	0.915 29	13
	0.6	1.200 40	0.596 09	0.990 56	0.862 29	13
	0.7	1.227 90	0.563 73	0.944 45	0.827 20	1.7
	0.8	1.269 16	0.523 14	0.954 94	0.792 24	1.0
	0.9	1.302 27	0.496 78	0.948 72	0.765 08	0.3
	1.0	1.337 84	0.471 30	0.952 17	0.738 55	1.3
3	0.1	1.025 65	0.894 94	1.044 03	1.149 40	0.8
	0.2	1.092 04	0.744 27	1.007 13	1.029 65	0.9
	0.3	1.156 49	0.639 91	0.940 29	0.906 67	1.9
	0.4	1.240 54	0.547 17	0.952 01	0.791 78	1.6
	0.5	1.311 65	0.484 89	0.932 78	0.708 47	3.0
	0.6	1.389 42	0.420 49	0.938 21	0.661 94	1.4
	0.7	1.454 72	0.375 54	0.921 75	0.625 47	1.3
	0.8	1.524 38	0.329 33	0.921 73	0.612 65	0.6
	0.9	1.589 54	0.293 55	0.922 90	0.608 44	2.5
	1.0	1.652 54	0.262 37	0.931 57	0.607 44	1.5
4	0.1	1.043 02	0.838 75	1.009 67	1.126 44	1.1
	0.2	1.147 18	0.657 82	0.967 76	0.922 22	1.0
	0.3	1.256 60	0.539 07	0.943 76	0.748 04	0.4
	0.4	1.370 26	0.440 08	0.934 04	0.647 74	0.7
	0.5	1.469 62	0.369 53	0.917 33	0.587 94	1.5
	0.6	1.566 50	0.315 55	0.906 86	0.547 08	0.9
	0.7	1.668 28	0.247 14	0.904 59	0.589 08	1.1
	0.8	1.759 33	0.215 62	0.896 48	0.565 56	1.4
	0.9	1.867 85	0.159 45	0.912 22	0.676 82	2.5
	1.0	1.950 94	0.130 86	0.910 94	0.760 60	6.3

We first consider the 2CLJ molecules for which $L^* = l^*$. The values of $B_{2CLJ}^*(T^*,L^*)$ were taken from Maitland et al.[7] and Boublík[8] for $0.1 \le l^* \le 0.6$ and from Boublík[8] for $0.7 \le l^* \le 1.0$. As shown in Figure 5, $B_{2CLJ}^*(T^*,L^*)$ does indeed display a nearly straight plot against the reference $B_0^*(T^*)$. Next, we determined r_m, ϵ, S_R, and S_A by a least-squares fit of the model $B(T)$ to $B_{2CLJ}^*(T^*,L^*)$. The resulting values of the parameters and the rms deviations from the numerical calculations are shown in Table 1. We find that the model reproduces $B_{2CLJ}^*(T^*,L^*)$ very accurately for all values of l^*. The rms deviations are at least an order of magnitude better than those obtained from a model based on spherocylindrical bodies.[8,9]

The depth $\epsilon^* = \epsilon/n^2\epsilon_{LJ}$ decreases smoothly with L^* and confirms the meaning of $\epsilon = \langle \epsilon_\Omega \rangle_\Omega$. This is apparent from Figure 6a, which shows the residual depth $\Delta\epsilon^*$ given by

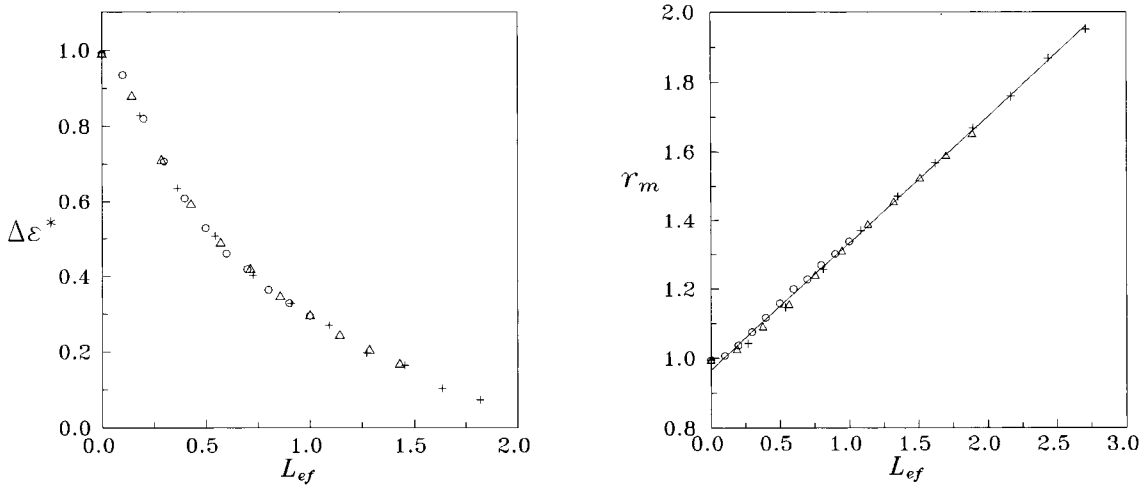

Figure 6. Parameters of the effective potential of the LJ polyatomics in terms of effective molecular elongation L_{ef}: (a) Reduced effective energy $\Delta\epsilon^*$, and (b) mean diameter r_m. Circles: diatomics. Triangles: triatomics. Crosses: tetratomics.

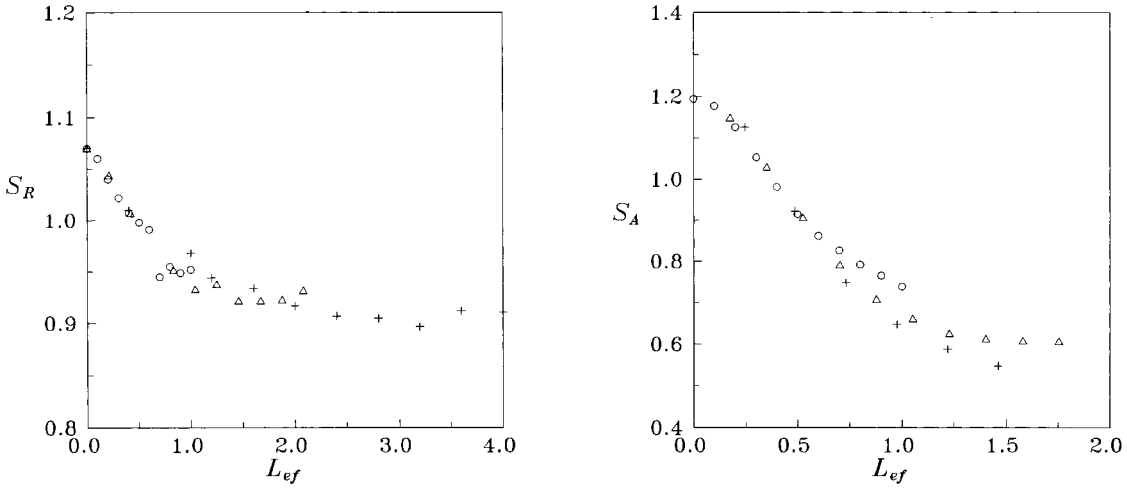

Figure 7. Softness parameters S_R and S_A of the LJ polyatomics. The symbols have the same meaning as in Figure 6.

$$\epsilon^* = \epsilon_\infty^*(n) + (1 - \epsilon_\infty^*)\Delta\epsilon^*$$

where $\epsilon_\infty^*(n = 2) = 0.25$. As shown in Figure 6b, $r_m^* = r_m/\sigma_{LJ}$ increases linearly with l^*. Last, the softness S_R and S_A also conform to the behavior already found for the linear Kihara molecules and shown in Figure 4: the longer molecules behave effectively as harder. This is shown in Figures 7a and b.

Hence, eqs 2.12, 2.13, and 2.1 give a very accurate and simple expression for $B_{2CLJ}^*(T^*,L^*)$. Since the 2CLJ system is quite common in applications, we also present in Table 1 the values of ϵ^*, r_m^*, S_R, and S_A for diatomics of various elongations.

We consider next the triatomic and tetratomic LJ molecules. The source of the $B_{nCLJ}^*(T^*,L^*)$ data is the calculation of Boublík.[8] The application of our model is similar as for the diatomics, although the confidence on the values of the parameters ϵ^*, r_m^*, S_R, and S_A, also shown in Table 1, is reduced due to the shorter range of available values of B_{nCLJ}^*, which for the larger values of l^* are all above the Boyle temperature. In all cases, the model developed here for $B(T)$ is able to reproduce the numerical data very accurately and the behavior of the parameters with l^* is as expected from the theory, except for the longer polyatomics where the errors in the parameters are larger.

The similitude of properties of different molecules with different shape but with equivalent elongations has been the subject of considerable interest. Indeed, we can find effective molecular elongations, $L_{ef}^* = (n - 1)l_n^*$, by which the similarities between the various LJ linear polyatomics are exhibited. The site−site effective elongation, l_n^*, is defined with respect to the 2CLJ site−site elongation l_2^* as $l_n^* = \kappa_n l_2^*$. For instance, in Figure 6a, the energies for different polyatomics are seen to scale by using $\kappa_3 = 0.7$ and $\kappa_4 = 0.55$. Nevertheless, the scaling constants κ_n are found to vary with the different properties. Figures 6 and 7 show also the parameters ϵ^*, r_m^*, S_R, and S_A for LJ triatomics and tetratomics where ϵ_∞^* and κ_n have the values shown in Table 2.

3.4. Square-Well Chains. Square-well chains furnish an example of long flexible molecules, and its second virial coefficient has been calculated recently by Wichert and Hall.[10] In this case, the repulsive interactions are accounted for by an effective hard sphere whose volume B_{hc} is obtained from the average excluded volume of chains of tangent hard spheres of diameter r_0. Hence, in our notation, $4b_m = B_{hc}(n)$, where n is the number of monomers in the chain, is independent of temperature. The effective σ_0 is then given by

TABLE 2: Effective Elongations for Multicentered LJ Molecules

n	ϵ_∞	κ_n (ϵ)	κ_n (r_m)	κ_n (S_R)	κ_n (S_A)
2	0.2500	1.00	1.0000	1.00	1.00
3	0.1111	0.70	0.5288	0.48	0.57
4	0.0625	0.55	0.3692	0.25	0.41

$$\sigma_0/r_0 = B_{hc}^*(n)^{1/3}$$

From the results of Yethiraj et al.,[11] due to the flexibility of the chains, r_m grows with n more slowly than the effective diameter of rigid chains. Since the repulsive part of the spherical effective potential is infinitely hard, we find that $S_R = 0$. The exact effective potential between two SW chains is then

$$u(r) = \begin{cases} \infty & r < \sigma_0 \\ -(k-j)\epsilon_0 & \sigma_j < r < \sigma_{j+1} \\ 0 & \sigma_k < r \end{cases}$$

where $j = 0, 1, 2, ..., k$, k gives the maximum number of site−site SW interactions, and each SW monomer has depth ϵ_0. The mean diameters σ_{j+1} are obtained from the distances at which $k-j$ SW overlap by averaging over all configurations. These averages can be deduced from the Monte Carlo results of Wichert and Hall.[10] The reduced exact effective potential $u_{ef}(z) = u(r/\sigma_0)/k\epsilon_0$ is shown in Figure 8 for $n = 2$ and 3.

Since the effective attractive potential has several steps, its contribution to the virial coefficient can be approximated by a smooth potential of the type $\omega_{MK}(z,n,S_A,a)$ which has a well-defined softness S_A with respect to the attractive part of the reference $u_0(z)$. The softness S_A and the effective depth ϵ^* are obtained in this approximation by fitting the attractive part (eq 2.13) to the corresponding part of the virial coefficient. The values of $\epsilon^*(n)$ and $S_A(n)$ for SW chains with range $\lambda_0 = 1.5$, obtained from $B(T)$ calculated by Wichert and Hall, are shown in Figure 9 and Table 3.

The resulting model is

$$B(T^*) = B_{hc}^*(n)\,[1 + S_A(1 - \Lambda_0^*(T^*))(e^{\beta\epsilon^*} - 1)] \quad (3.21)$$

where $T^* = kT/\epsilon^*$, the core contribution $B_{hc}^*(n)$ is given by Wichert and Hall, and $\Lambda_0^*(T^*)$ is the reference attractive volume. Using the values of $\epsilon(n)$ and $S_A(n)$ from Table 3 in eq 3.21, we obtain good agreement with the Monte Carlo results, even below the Boyle temperature, as shown in Figure 10 in terms of the reduced temperature $T_0^* = kT/\epsilon_0$. From Figure 9a

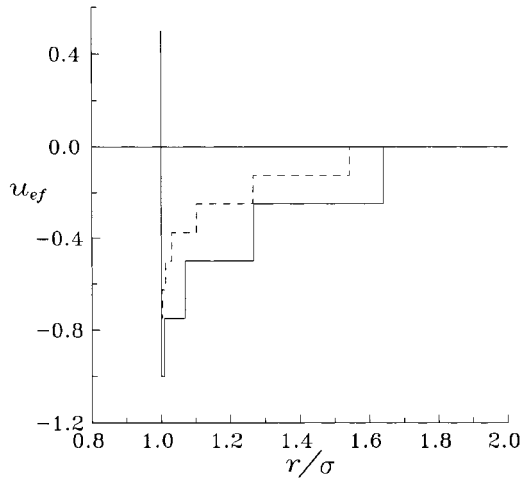

Figure 8. Exact effective potentials for square-well chains: solid line, $n = 2$; dashed line, $n = 3$.

we notice that, as in the case of the rigid linear LJ polyatomics, ϵ^* increases with the length of the chain and the maximum number of SW overlaps, although an asymptotic behavior is apparent for large n. As can be inferred from the effective potentials in Figure 8, the smoothed effective potential is quite steep and becomes steeper, i.e., harder for the longer chains. The softness S_A shown in Figure 9b is noticeably smaller than the attractive softness of the rigid linear molecules considered in the previous sections, although it has a similar qualitative behavior with length.

3.5. Polar Molecules. A final test of the theory was made for a simple polar model, given by the well-known Stockmayer potential $u_{ST}(r,\Omega)$ constructed by the addition of a dipole−dipole term to a LJ12/6 potential function. Since the profile of $u_{ST}(r,\Omega)$ against r can present two minima at some orientations, the theory developed in section 1 applies only as an approximation and only in cases where the dipole strength δ_{max} given by

$$\delta_{max} = \frac{\mu^2}{2\epsilon\,(\sigma^3 4\pi\epsilon_0)}$$

is not too large. The virial coefficient of this model has been studied by several authors and is tabulated by Maitland et al. as a function of the temperature reduced with the LJ potential depth $T_{LJ}^* = kT/\epsilon_{LJ}$.[7] Again, a least-squares fit of the model $B^*(T^*,S_R,S_A)$ to the tabulated values of $B_{ST}^*(T_{LJ}^*)$ shows that

TABLE 3: Parameters for the Effective Potentials of SW Chains

n	ϵ^*	S_A	T_{B_0}
2	3.632 42	0.279 105	3.040
3	4.535 06	0.212 806	3.089
4	5.390 57	0.166 297	3.097
8	7.653 70	0.091 021 4	3.096
16	9.699 62	0.051 683 0	3.034
24	10.849 8	0.408 279 0	3.100
50	12.026 4	0.034 489 3	3.250

TABLE 4: Parameters for the Effective Potentials of Stockmayer Molecules

δ_{max}	r_m	ϵ	S_R	S_A	Q	ΔT^*
0.25	0.908 64	1.231 66	0.759 13	1.242 18	0.170	0.3−25
0.50	0.870 29	1.670 48	0.589 38	1.025 53	0.220	0.4−25
1.00	0.851 93	2.743 05	0.465 39	0.699 48	0.024	0.6−20
2.00	0.840 83	5.249 07	0.356 81	0.467 70	0.034	1.0−25

eqs 2.12 and 2.13 hold to a good approximation from quite low temperatures up to the inversion temperature where $B_{ST}^*(T_{LJ}^*)$ shows a maximum. Figure 11 shows plots for the deviations between the theoretical values and the ones calculated numerically, $\Delta B^*(T_{LJ}^*) = B_{num}^*(T_{LJ}^*) - B_{theo}^*(T_{LJ}^*)$. These deviations are seen to be small. The values for the effective parameters ϵ, r_m, S_R, and S_A are shown in Figure 11. These values are tabulated in Table 4 together with the mean rms deviation Q and the temperature interval ΔT_{LJ}^* for each dipolar strength considered. Last, the behavior of the effective parameters of the Stockmayer molecules is shown in Figure 12. The effective depth ϵ increases almost proportionaly to δ_{max}, and the predominant attractive configurations make the effective size r_m decrease slightly. In general, both parts of the effective potential tend to appear harder as δ_{max} increases and the Stockmayer potential deviates more and more from sphericity; nevertheless, the repulsive softness S_R has a small maximum around $\delta_{max} \simeq 0.25$.

4. Conclusions

The theory of effective potentials based on softness parameters is shown to provide an excellent account of the virial coefficients of a variety of nonspherical potential models. With the scale and form parameters found in this work, one can not only calculate simply and accurately the corresponding virial coefficients, but also construct the effective spherical potentials in the gas phase. Hence, this theory is able to take into account

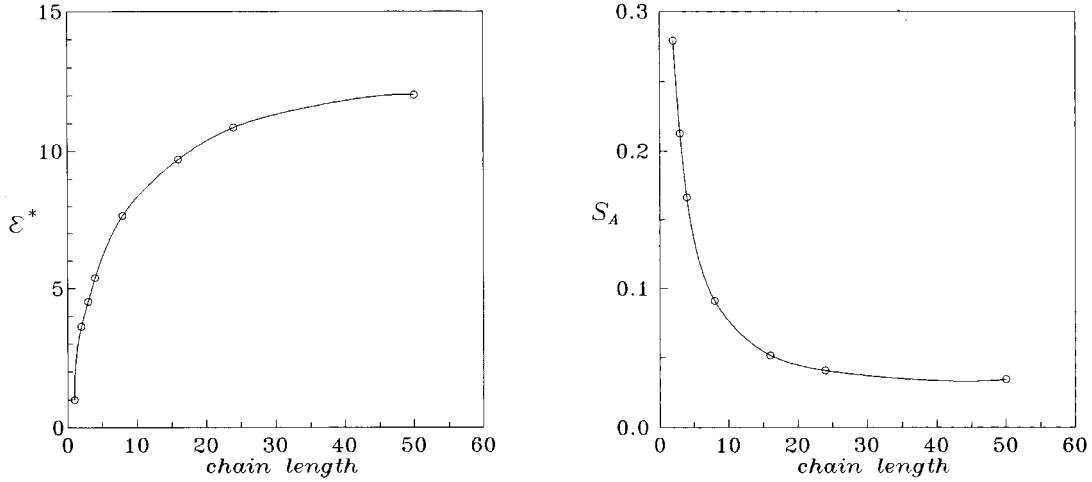

Figure 9. Parameters of the attractive effective potential of SW chains in terms of chain length: (a) effective energy ϵ^*, and (b) softness S_A. Circles: results from the theory. The solid lines are drawn to guide the eye.

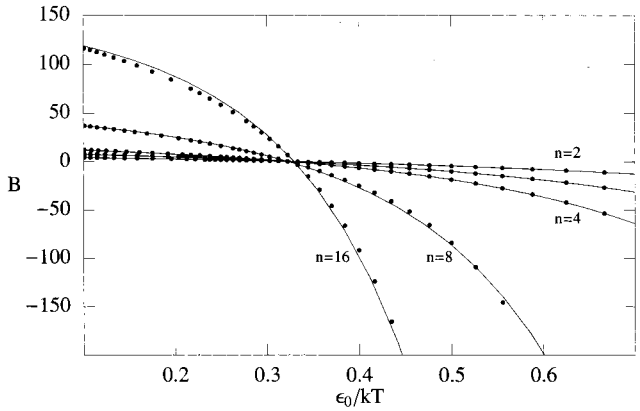

Figure 10. Virial coefficient of SW chains. Solid circles show the results of Wiechert and Hall Monte Carlo simulations,[10] and the solid lines represent the results of this work. The lines are labeled by the length of the chain, except for the $n = 3$ case which lays between the $n = 2$ and the $n = 4$ cases.

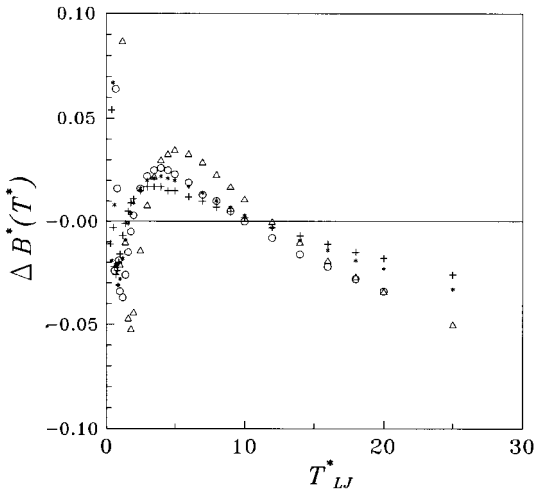

Figure 11. Deviation plot for the virial coefficient of Stockmayer molecules. $\Delta B^*(T_{LJ}^*) = B_{num}^*(T_{LJ}^*) - B_{theo}^*(T_{LJ}^*)$ where $B_{theo}^*(T^*) = B^*(T^*, S_R, S_A)$ as given by this theory with ϵ, S_R, and S_A taken from Table 4. The points correspond to different values of the dipolar strength: $\delta_{max} = 0.25$ (+), $\delta_{max} = 0.5$ (*), $\delta_{max} = 1.0$ (○), and $\delta_{max} = 2.0$ (△).

deviations from nonconformality due to differences in the form of the potential profile and/or the shape of the molecules.

In particular, we find that the shape of a molecule affects its repulsive and attractive softnesses, S_R and S_A, so that elongated molecules appear as effectively harder, i.e., the longer molecules have steeper effective potentials. Different models of linear molecules produce different quantitative behaviors of S_R and S_A with elongation, although the qualitative trends are similar. For potential models with a constant well's depth, the effect of the attractive forces is seen to diminish with elongation or, more generally, eccentricity.

Application of this theory to real gases will be the subject of forthcoming papers.

Acknowledgment. I. A. McLure and F. del Río acknowledge support from the European Commission through Contract No CI1*CT94-0132 and from the Consejo Nacional de Ciencia y Tecnología (México) through Grant No. 400200-5-1400PE. J. E. Ramos is thankful to Conacyt (México) for support. Dr. D. C. Williamson contributed with meanignful discussions and comments.

5. Appendix

5.1. Linear Kihara Molecules. We start from a general discontinuous potential from which one can obtain the continuous case as a limit. Consider a potential constituted by coaxial spherocylindrical shells at $r = r_n(\Omega)$ such that

$$u(r,\Omega) = \begin{cases} \infty & r < r_1(\Omega) \\ \epsilon_n \quad r_n(\Omega) < r < r_{n+1}(\Omega), \text{ for } n \geq 1 & \\ 0 & r_c(\Omega) < r \end{cases}$$

so that ϵ_n is the height of the potential for $r_n < r < r_{n+1}$, s_{00} is the core thickness, and $\epsilon_0 = \infty$. The potential steps are repulsive for $0 \leq n \leq M$ and attractive for $M + 1 < n \leq c$. The minimum value of the potential is $\epsilon_m < 1$, and all heights ϵ_n are angle independent. The Boltzmann factor in eqs 2.5 and 2.6 is

$$e^{-\beta u(r,\Omega)} = \sum_{n=0}^{c} H(r - r_n(\Omega))(e^{-\beta\epsilon_{n+1}} - e^{-\beta\epsilon_n})$$

so that the force is proportional to

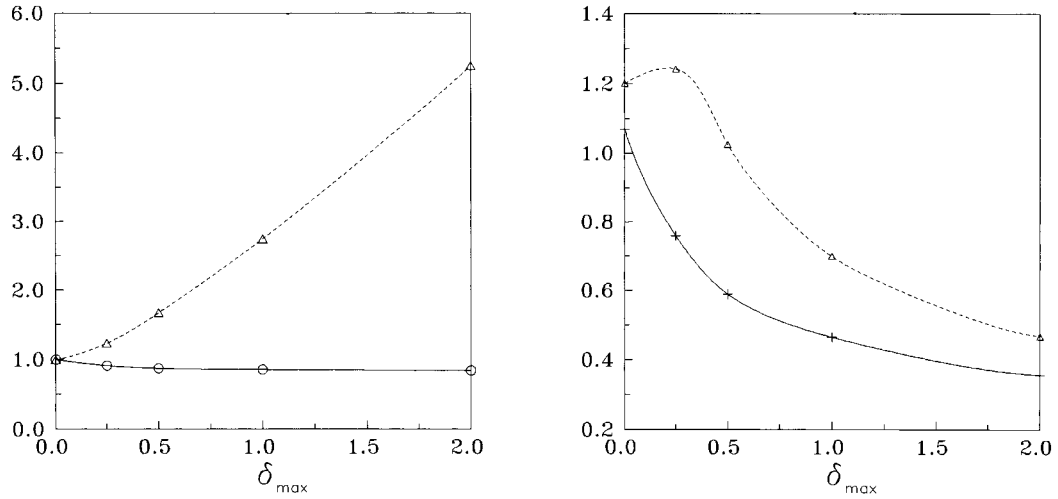

Figure 12. Effective molecular parameters for Stockmayer molecules as function of the dipolar strength: (a) effective depth ϵ (△) and diameter r_m (○); (b) repulsive S_R (△) and attractive S_A (+) softnesses.

$$\frac{\partial e^{-\beta u(r,\Omega)}}{\partial r} = \sum_{n=0}^{c} \delta(r - r_n(\Omega))\,(e^{-\beta\epsilon_{n+1}} - e^{-\beta\epsilon_n})$$

and integrating over the angles, the mean collision diameters are found to be

$$\sigma^3 e^{\beta\epsilon} = \sum_{n=0}^{M} b_n b_{hsc}^*(L_n^*)(e^{-\beta\epsilon_{n+1}} - e^{-\beta\epsilon_n})$$

and

$$R^3(e^{\beta\epsilon} - 1) = -\sum_{n=M+1}^{c} b_n b_{hsc}^*(L_n^*)(e^{-\beta\epsilon_{n+1}} - e^{-\beta\epsilon_n})$$

where $b_n = r_{n_0}{}^3$ and r_{n_0} is the thickness of the nth SC shell. Now

$$b_n b_{hsc}^*(L_n^*) = r_{n0}{}^3 + \frac{3}{2}L r_{n0}{}^2 + \frac{3}{8}L^2 r_{n0}$$

We now take the limit of infinitely many steps $M \to \infty$ and $c \to \infty$, with $\delta r = r_{n+1} - r_n$, $\delta\epsilon = \epsilon_{n+1} - \epsilon_n \to 0$, so that $r_M = r_{M+1} = r_m$ constant

$$\sigma^3 e^{\beta\epsilon} = \int_{r_0}^{r_m} dr f(r,L) \frac{\partial e^{-\beta u(r)}}{\partial r}$$

and

$$R^3(e^{\beta\epsilon} - 1) = -\int_{r_m}^{\infty} dr\, f(r,L) \frac{\partial e^{-\beta u(r)}}{\partial r}$$

where $u(r)$ is the continuous potential between two spherical particles and

$$f(r,L) = r^3 + 3Lr^2/2 + 3L^2 r/8$$

If we set the main elongation L^* equal to L/r_m, then

$$\sigma_{sc}{}^3/r_m{}^3 = b_0^*(T^*) + \frac{3}{2}L^* b_1^*(T^*) + \frac{3}{8}L^{*2} b_2^*(T^*)$$

and

$$R_{sc}{}^3/r_m{}^3 = \Lambda_0^*(T^*) + \frac{3}{2}L^*\Lambda_1^*(T^*) + \frac{3}{8}L^{*2}\Lambda_2^*(T^*)$$

with $b_k^*(T^*)$ and $\Lambda_k^*(T^*)$ given in the main text. For $k = 0$, these functions are the effective volumes of the $L = 0$ SSC: $b_0(T^*) = b_{sc}^*(T^*, L^* = 0)$ and $\Lambda_0(T^*) = \Lambda_{sc}^*(T^*, L^* = 0)$. Integrating the integrals in the last two equations by parts, we find that in the $T^* \to 0$ limit

$$b_{30}^* = b_{20}^* = b_{10}^* = 1$$

and

$$\Lambda_{30}^* = \Lambda_{20}^* = \Lambda_{10}^* = 1$$

Hence, at $T^* = 0$, the effective volumes are equal

$$\sigma_{sc}{}^3/r_m{}^3 = R_{sc}{}^3/r_m{}^3 = 1 + \frac{3}{2}L^* + \frac{3}{8}L^{*2} = b_{hsc}^*(L^*)$$

The normalized SC volume is then

$$b_{sc}^*(T^*,L^*) = \frac{1}{b_{hsc}^*(L^*)}(\sigma_{sc}/r_m)^3 = \frac{1}{b_{hsc}^*(L^*)}\left[b_3^*(T^*) + \frac{3}{2}L^* b_2^*(T^*) + \frac{3}{8}L^{*2} b_1^*(T^*)\right]$$

In the limit of long elongation

$$b_{sc}^*(T^*, L^* \to \infty) = b_1^*(T^*)$$

The softness in this limit is the slope of the approximate straight line obtained from a parametric plot of $b_1^*(T^*)$ against $b_3^*(T^*)$ and depends on the potential $u(r)$. Similarly, one finds that the normalized SC attractive volume is

$$\Lambda_{sc}^*(T^*,L^*) = \frac{1}{b_{hsc}^*(L^*)}(R_{sc}/r_m)^3 = \frac{1}{b_{hsc}^*(L^*)}\left[\Lambda_3^*(T^*) + \frac{3}{2}L^*\Lambda_2^*(T^*) + \frac{3}{8}L^{*2}\Lambda_1^*(T^*)\right]$$

and thus

$$\Lambda_{sc}^*(T^*, L^* \to \infty) = \Lambda_1^*(T^*)$$

References and Notes

(1) del Río, F.; Ramos, J. E.; McLure, I. A. *J. Phys. Chem.* **1998**, in press.
(2) del Río, F.; Ramos, J. E.; Gil-Villegas, A.; McLure, I. A. *J. Phys. Chem.* **1996**, *100*, 9104.
(3) Frisch, H. L.; Helfand, E. *J. Phys. Chem.* **1960**, *32*, 269.
(4) Cox, H. E.; Crawford, F. W.; Smith, E. B.; Tindell, A. R. *Mol. Phys.* **1980**, *40*, 705.
(5) Kihara, T. *Intermolecular Forces*; John Wiley: New York, 1978.
(6) Boublík, T.; Nezbeda, I. *Coll. Czech. Chem. Commun.* **1986**, *51*, 2301.
(7) Maitland, G. C.; Rigby, M.; Smith, E. B.; Wakeham, W. A. *Intermolecular Forces*; Oxford: New York, 1981.
(8) Boublík, T. *Coll. Czech. Chem. Commun.* **1994**, *59*, 756.
(9) Boublík, T. *Mol. Phys*. **1983**, *49*, 675.
(10) Wichert, J. M.; Hall, C. K. *Macromolecules* **1994**, *27*, 2744.
(11) Yethiraj, A.; Honnel, K. G.; Hall, C. K. *Macromolecules* **1992**, *25*, 3979.